Rotational Behavior of *N*-(2-Naphthylmethyl)carbazole in a 1,2-Dichloroethane/Poly(ethylene oxide) Mixture Measured by a Time-Resolved Fluorescence Depolarization Method

Fumiaki Tsunomori* **and Hideharu Ushiki**

Graduate School of Bio-Applications and Systems Engineering, Tokyo University of Agriculture and Technology, Fuchu, Tokyo 183

(Received December 20, 1995)

Stationary and nanosecond time-resolved fluorescence depolarization spectroscopy has been used to detect the rotational behavior of *N*-(2-naphthylmethyl)carbazole as a function of the solvent viscosity. The variation in the viscosity was effected by the addition of poly(ethylene oxide), and the range of the variation was 0.78 N m^{-2} s^{-1} to 33×10^{-3} N m^{-2} s^{-1}. The viscosity dependence of the rotational diffusion coefficient (D_r) in the high-viscosity region was different from that in the low viscosity region. Radii of gyration of *N*-(2-naphtylmethyl)carbazole in the low and high viscosity regions were about 8 and 4 Å, respectively. The former agrees with the total size of *N*-(2-naphthylmethyl)carbazole, and the latter with the size of the cabazolyl group. The crossover point of the rotational motion of *N*-(2-naphthylmethyl)carbazole was at a concentration of 0.6 g ml^{-1} of poly(ethylene oxide), which coincided with the overlap concentration of poly(ethylene oxide) molecules. Therefore, the rotational mode of *N*-(2-naphthylmethyl)carbazole varies from the whole to the carbazolyl group by the addition of poly(ethylene oxide).

The rotational behavior of solute molecules dissolved in an amorphous system reflects the microscopic structure and/or environment of the system.[1] Generally, the rotational motion of solute molecules is discussed on the basis of the Stokes–Einstein–Debye theory.[2—4] According to this theory, solute molecules can rotate with the friction (ζ) as

$$\zeta = 6\eta VfB, \tag{1}$$

where η, V, f, and B are the solvent viscosity, volume of a solute molecule, the shape factor, and a parameter which depends on the boundary condition, respectively. The shape factor is determined by the ellipsoidal axial ratio of a solute molecule. The value of f is larger than unity in the case of a non-sphere approximation; if a solute molecule is spherical the shape factor (f) is 1. Parameter B is unity in the "stick" limit condition, which refers to treating the surrounding medium as a continuum. In the "subslip" and "slip" conditions, which imply the solvent cavity, B can take a value between 1 and 0.

The rotational friction (ζ) is related to the rotational diffusion coefficient (D_r) and the rotational correlation time (θ) as

$$D_r = \frac{1}{6\theta} = \frac{k_B T}{\zeta}, \tag{2}$$

where k_B and T are the Boltzmann constant and the absolute temperature, respectively. By substituting Eq. 1 in Eq. 2, one can obtain

$$D_r = \frac{k_B T}{6\eta VfB}. \tag{3}$$

The fluorescence depolarization technique enables us to obtain the rotational diffusion coefficient (D_r) of a molecule and/or a functional group by a stationary and time-resolved measurement. The former is based on the well-known Perrin's equation,[5]

$$\frac{1}{\bar{r}} = \frac{1}{r_0}\left(1 + \frac{\tau_f}{6D_r}\right), \tag{4}$$

where $\bar{r}$, r_0, and τ_f are the mean anisotropy ratio calculated using the fluorescence anisotropy spectrum, a constant as the anisotropy ratio in a rigid solution, and the excited singlet lifetime, respectively. Thus, $\bar{r}$ and τ_f are required. The latter provides the time evolution of the anisotropy ratio ($r(t)$), which implies valuable information about the interaction between a solute and solvent molecules. By a primary treatment, $r(t)$ is analyzed by a single exponential function as

$$r(t) = r_0 \exp(-6D_r t). \tag{5}$$

Hence, we can directly obtain D_r.

Cicerone and Ediger[6] have discussed the heterogeneous dynamic domains of *ortho*-terphenyl near T_g via the temperature dependence of the rotational correlation time of tetracene, measured by the photobleaching technique. They suggested a relationship between the rotation of solute molecules and the structure of the grass system. Brocklehurst and Young[7] have reported on the non-hydrodynamic behavior of perylene in squalene and methylcyclohexane systems based on the nanosecond single-photon counting method. They have pointed out that the size of a solute molecule relative to that of a solvent molecule is important concerning the

rotational behavior of solute molecules, and have discussed about the contribution of the shape factor to the rotational motion. The solvation effect for the rotational motion of rose bengal in a binary mixture was investigated by Srivastava and Doraiswamy[8] on the basis of the picosecond single-photon counting technique. They, however, concluded that the effect of a variation in the boundary condition cannot be found on the rotational dynamics of solute molecules.

In this paper, we report on the rotational behavior of *N*-(2-naphthylmethyl)carbazole in 1,2-dichloroethane and poly(ethylene oxide) mixtures at 30 °C.

Experimental

A. Materials. *N*-(2-Naphthylmethyl)carbazole (NMC) was synthesized by a reaction of potassium carbazolide with 2-chloromethylnaphthalene.[9] Potassium hydroxide (1.0 g) was added to carbazole (2.5 g) dissolved in tetralin (15 ml) with xylene (7.5 ml). The mixture was vigorously stirred at 150 °C for about two hours to be transformed to a yellow suspension of potassium carbazolide. The water formed was azeotroped off with xylene. 2-chloromethylnaphthalene was added to potassium carbazolide, and the mixture heated to 170 °C for about seven hours. After the mixture was allowed to stand at room temperature, potassium carbazolide was filtrated off, and the solvents removed from the filtrated by a rotatory evaporator. The product was a white powder after recrystallization once from benzene and several times from ethanol. This compound was identified as NMC based on disappearance of N–H absorption in the infrared spectrum, and confirmed to be pure by thin-layer chromatography. The molecular structure of NMC is shown in Fig. 1.

Poly(ethylene oxide), whose molecular weight is about 300 (PEO300), and 1,2-dichloroethane were purchased from Wako Chemical Co., and used as received.

B. Method. NMC were dissolved in a mixed solvent of PEO300 and 1,2-dichloroethane at a concentration of 1.0×10^{-7} mol dm^{-3}. The solvent viscosity changed by the fraction volume of PEO300 was in the range from 0.78×10^{-3} to 33×10^{-3} N m^{-2} s^{-1}. The samples were deaerated by several freeze-pump-thaw cycles under a high-vacuum system, and sealed in a cylindrical cell of 1 cm diameter.

The viscosities of the mixed solvent were measured using an Ubbelohde viscometer at 30 °C. The concentration of PEO300 was determined based on the volume fraction of PEO300 and the specific gravity of PEO300 measured with a pycnometer at 30 °C. The specific gravity of PEO300 at 30 °C was 1.13 g ml^{-1}.

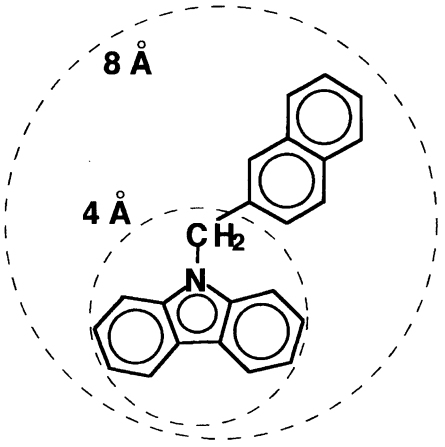

Fig. 1. Molecular structure of *N*-(2-naphthylmethyl)carbazole.

The emission spectra of NMC with polarization parallel and perpendicular to that of the exciting light were recorded using a fluorescence spectrophotometer (Hitachi 650-60) with polarizing filters (Hitachi 650-0155). In order to excite the carbazolyl group selectively, the excitation wavelength was 340 nm.

The fluorescence decay curve and the polarized fluorescence decay curve of NMC excited at 340 nm were measured by a nanosecond time-resolved fluorescence spectroscopy using a time-correlated single-photon counting method (Horiba NAES-1100). The fluorescence intensity was observed through a sharp cut filter (Toshiba UV35).

All of the spectroscopic measurements were carried out at 30 °C.

Results and Discussion

A. Fluorescence Anisotropy Ratio. The fluorescence depolarization spectra of NMC were calculated using

$$r(\lambda)=\frac{I_{VV}(\lambda)-GI_{VH}(\lambda)}{I_{VV}(\lambda)+2GI_{VH}(\lambda)}, \tag{6}$$

where λ and G are the wavelength and compensating factor of the anisotropic sensitivity of the apparatus. The factor G is defined as $G\equiv I_{HV}/I_{HH}$. $I_{VV}(\lambda)$, $I_{VH}(\lambda)$, $I_{HH}(\lambda)$, and $I_{HV}(\lambda)$ denote the polarized fluorescence intensities. Subscripts V and H represent the parallel and perpendicular direction to the vertical line. The first suffix indicates the direction of the incident light and the second the emitted light.

The inset of Fig. 2 shows the fluorescence and anisotropy spectra at $\eta=3.7\times10^{-3}$ N m^{-2} s^{-1}. The large value of r at the left edge of the spectrum ($\lambda<360$ nm) is because that the monitor wavelength was close to the excitation one. According to Eq. 6, when the monitor wavelength is close to that of excitation, the value of I_{VV} is much larger than that of I_{VH} because of the scattering of the excitation light, so that the value of r becomes large. In the range over 400 nm wavelength, the value of the anisotropy r increases with increasing wavelength, because this area is the base of the spectrum. In this region, since the value of I_{VH} is much smaller than that of I_{VV}, the value of r is also large, because of an increase in the error in the fluorescence intensity. We therefore evaluate the mean fluorescence anisotropy ratio ($\bar{r}$) using

$$\bar{r}=\frac{1}{\lambda_2-\lambda_1+1}\int_{\lambda_1}^{\lambda_2} r(\lambda)\mathrm{d}\lambda, \tag{7}$$

where λ_1 and λ_2 are the cut-off wavelengths of the lower and upper limits. We adopted $\lambda_1=360$ nm and $\lambda_2=400$ nm, respectively. The viscosity dependence of $\bar{r}$ is shown in Fig. 2. The value of $\bar{r}$ increases linearly with the solvent viscosity.

B. Fluorescence Lifetime. The fluorescence decay curves of NMC for various viscosities of the solvent were analyzed using a single-exponential function as the true decay function:

$$S(t)=S_0\exp\left(-\frac{t}{\tau_f}\right), \tag{8}$$

where S_0 and τ_f are the intensity of fluorescence at $t=0$ and the excited singlet lifetime of NMC. The fluorescence decay

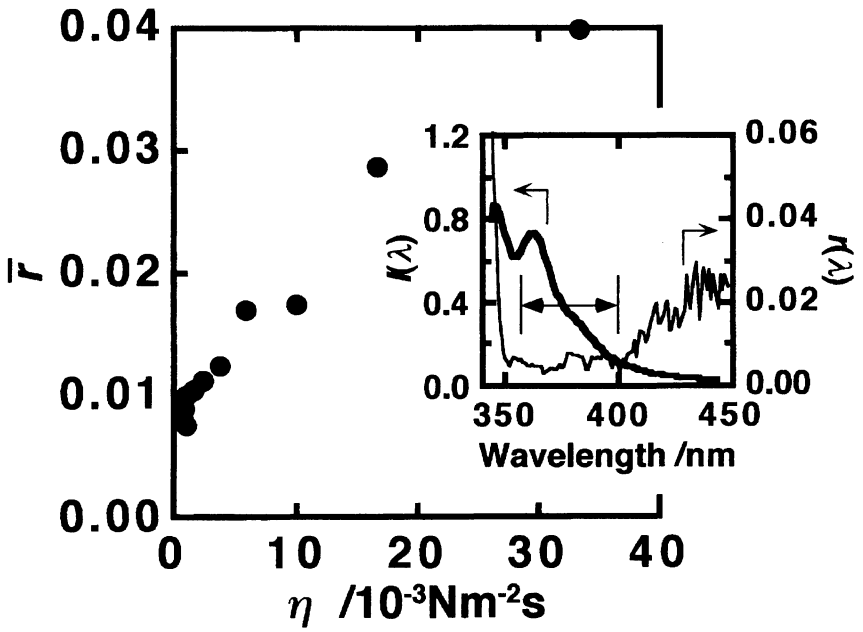

Fig. 2. Mean fluorescence anisotropy ratio $\bar{r}$ dependent on the solvent viscosity η. Inset indicate the emission and the fluorescence anisotropy spectra of NMC at η=3.7×10^{-3} N m^{-2} s^{-1}. The values of $\bar{r}$ are calculated by Eq. 7.

($I_{cal}(t)$) were reproduced by

$$I_{cal}(t) \approx \int_0^t P(T)S(t-T)\mathrm{d}T, \tag{9}$$

where $P(t)$ denotes the response function of the apparatus. Deconvolution and a curve-fitting calculation were carried out on the basis of Wahl's method[10] and the quasi-Marquardt algorithm,[11] respectively. The suitability of the function to data was evaluated by a value of the residual sum of squares (χ^2):

$$\chi^2 = \frac{1}{t_2 - t_1 - 2}\int_{t_1}^{t_2} w(t)[I_{obs}(t) - I_{cal}(t)]^2\mathrm{d}t, \tag{10}$$

where t_1, t_2, $w(t)$, and $I_{obs}(t)$ are the lower and upper cut-off times for the calculation, a weight function at time t, and the observed fluorescence-decay data, respectively. The weight function adopted for $I_{cal}(t)$ is

$$w(t) = \frac{1}{I_{obs}(t)}. \tag{11}$$

Adequate values of the variable parameters, I_0 and τ_f, were computed until the variation of χ^2 become less than 1×10^{-6}. The fluorescence-decay curve of NMC molecules and the profile of $P(t)$ are shown in Fig. 3 by the filled circles and solid line, respectively. The fluorescence-decay curves of NMC molecules were well fitted by a single exponential function. Figure 4 shows the solvent-viscosity dependence of the excited singlet lifetime of NMC (τ_f). In the range η<6×10^{-3} N m^{-2} s^{-1}, the value of τ_f tends to decrease with the solvent viscosity. On the other hand, in the range η>6×10^{-3} N m^{-2} s^{-1}, the value of τ_f is constant at about 3 ns.

Figure 5 shows the excitation spectra of NMC dependent on the solvent viscosity. The excitation spectra plotted in Fig. 5 are normalized in such the way that

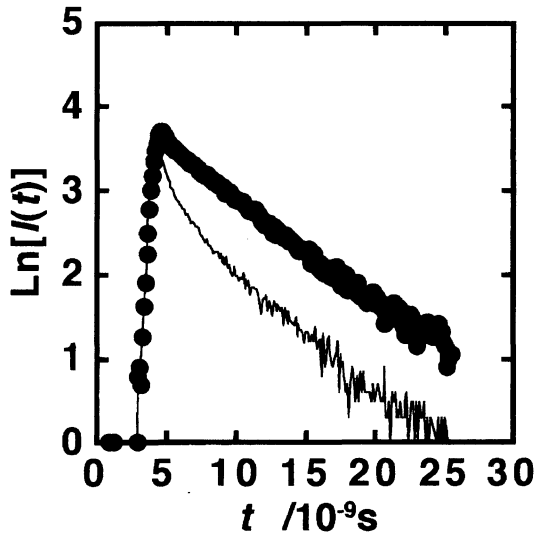

Fig. 3. Fluorescence decay curve of NMC molecules excited by wavelength of 340 nm, which can excite selectively the carbazolyl group in NMC molecule, at η=3.7×10^{-3} N m^{-2} s^{-1}.

$$\int_{250}^{370} E(\lambda)\mathrm{d}\lambda = 1, \tag{12}$$

where $E(\lambda)$ is the excitation spectrum. The absorption band of the carbazolyl group in the NMC molecule is in the 320 to 360 nm range. The peak around 290 nm probably corresponds to the absorption band of the naphthyl group in NMC. The profiles were obviously changed by the addition of PEO300 molecules. The excitation intensity at 340 nm as an indication of the absorption band of the carbazolyl group increased with increasing the amount of PEO300 in the range η<6×10^{-3} N m^{-2} s^{-1}. On the other hand, in the range η>6×10^{-3} N m^{-2} s^{-1}, the excitation intensity at 340

nm tends to be constant.

Therefore, the decrease in the singlet excited lifetime (τ_f) in the range $\eta<6\times10^{-3}$ N m^{-2} s^{-1} is due to a variation in the excited state of the carbazolyl group with the PEO300 molecule. In the range $\eta>6\times10^{-3}$ N m^{-2} s^{-1}, since the interaction between the excited carbazolyl group and PEO300 become stationary, the value of τ_f becomes constant.

C. Radius of Gyration of NMC by Stationary Measurement. Figure 6 shows the rotational diffusion coefficient (D_r) of NMC, which is dependent on the reciprocal of the solvent viscosity. The solvent viscosity dependence of D_r is obviously divided into two regions; the crossover point is estimated as $\eta^{-1}=1.6\times10^2$ m^2 (Ns)$^{-1}$. In Eq. 4, the value of r_0 had been determined to be 0.232 in glycerol-water mixed system.[12]

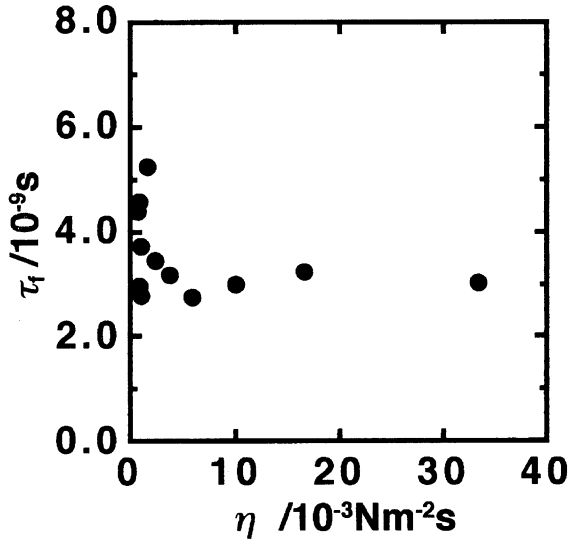

Fig. 4. The viscosity dependence of the single excited lifetime τ_f of NMC excited by wavelength of 340 nm.

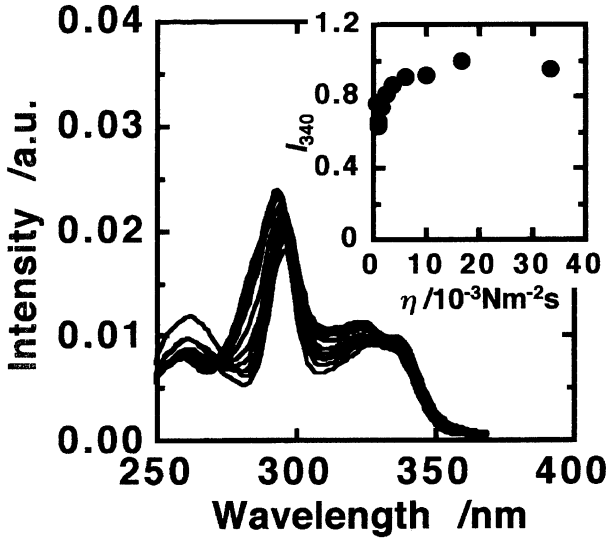

Fig. 5. Excitation spectra of NMC monitored at 370 nm. Inset indicate the viscosity dependence of the excitation intensity at 340 nm.

The slopes of the line in the low- and high-viscosity regions are 2.8×10^5 J m^{-3} and 3.9×10^6 J m^{-3}, respectively. Assuming the shape factor (f) of 1 and a "stick" limit approximation (B) of 1, the slope of the line in Fig. 6 represent the volume of NMC as a rotator. The radii of gyrations of NMC in the low- and the high-viscosity regions are roughly evaluated as 8.4 and 3.5 Å, respectively.

D. Radius of Gyration of NMC by a Time-Resolved Measurement. The fluorescence anisotropy decay curves ($r_{obs}(t)$) shown in Fig. 7 were calculated using

$$r_{obs}(t)\equiv\frac{I_{VV}(t)-GI_{VH}(t)}{I_{VV}(t)+2GI_{VH}(t)}. \quad (13)$$

The subscripts have the same meanings as in the above section. The fluorescence anisotropy decay ($r_{cal}(t)$) is reproduced by

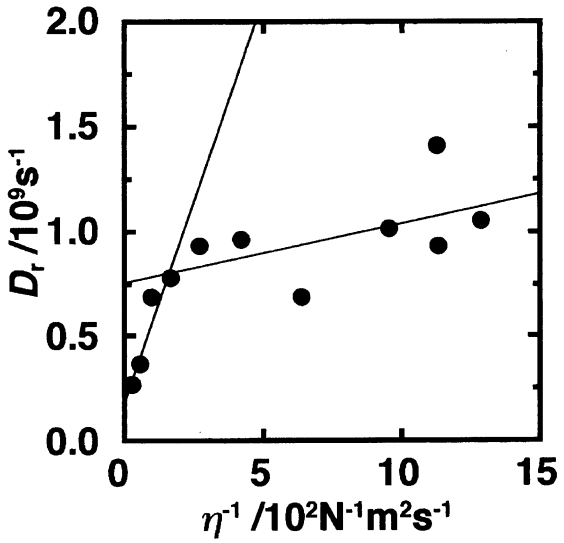

Fig. 6. The viscosity dependence of the rotational diffusion coefficient D_r of NMC, which are evaluated by Eq. 4. Two lines are drawn based on the least square fitting.

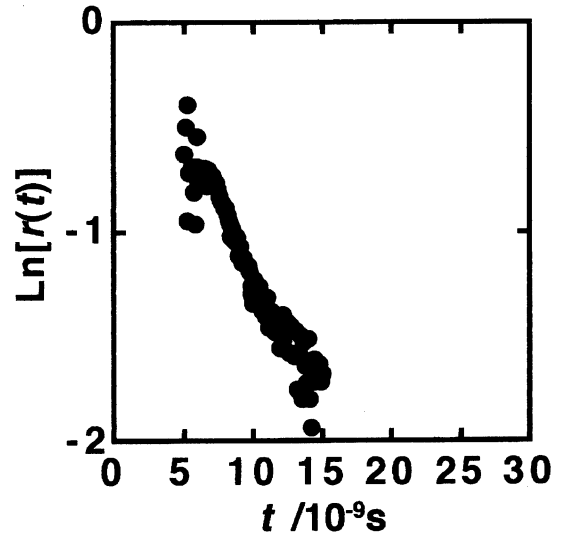

Fig. 7. Fluorescence anisotropy decay curve of NMC molecules at $\eta=3.7\times10^{-3}$ N m^{-2} s^{-1}.

$$r_{cal}(t) \approx \frac{\int_0^t P(T)S(t-T)r(t-T)dT}{\int_0^t P(T)S(t-T)dT}. \quad (14)$$

Though we used $S(t)$ as a single exponential function in the above section, in this section we assumed that $S(t)$ may be a biexponential function. Upon fitting data with $S(t)$, χ^2 was calculated using

$$\chi^2 = \frac{1}{t_2 - t_1 - 4}\int_{t_1}^{t_2} w(t)[I_{obs}(t) - I_{cal}(t)]^2 dt, \quad (15)$$

The weight function adopted for $I_{cal}(t)$ was

$$w(t) = \frac{1}{I_{VV}(t) + 4G^2 I_{VH}(t)}. \quad (16)$$

Upon evaluating the parameters in $r(t)$, Eq. 10 was substituted by

$$\chi^2 = \frac{1}{t_2 - t_1 - 2}\int_{t_1}^{t_2} w(t)[r_{obs}(t) - r_{cal}(t)]^2 dt, \quad (17)$$

The weighting function was replaced by

$$w(t) = \frac{3I_{obs}(t)}{1 + G + 3Gr_{obs}(t) - 3r_{obs}(t)^2 - 2(2G-1)r_{obs}(t)^3}, \quad (18)$$

according to Wahl.[10]

If the rotator in solution is a rigid sphere ($f=1$), a fluorescence-anisotropy decay curve is described by a single exponential function, as Eq. 5. Figure 8 shows the rotational diffusion coefficient, which is dependent on the reciprocal of the solvent viscosity. Evidently the solvent-viscosity dependence of D_r is divided into two regions; the crossover point is estimated to be $\eta^{-1}=2.0\times10^2$ m^2 (Ns)$^{-1}$. The slopes of the line in the low- and high-viscosity regions is 3.8×10^5 and 1.7×10^5 J m^{-3}, respectively. Therefore, the radius of gyrations of NMC in the low- and high-viscosity regions is roughly evaluated as 7.6 and 4.6 Å, respectively.

The radii of gyrations of NMC, obtained by stationary and time-resolved measurements, are summarized in Table 1.

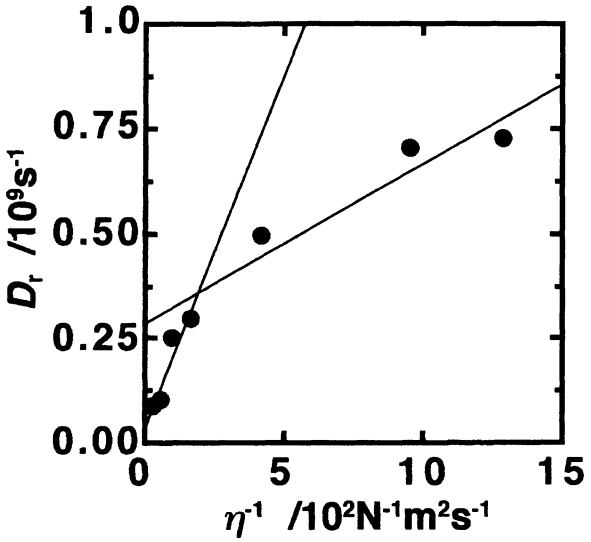

Fig. 8. The viscosity dependence of the rotational diffusion coefficient D_r of NMC, which are evaluated by Eq. 5. Two lines are drawn based on the least square fitting.

Table 1. Radius Gyrations (Å) of NMC in 1,2-Dichloroethane/Poly(ethylene oxide) Mixture, Obtained by Stationary and Time-Resolved Measurements

Method	Region	
	Low η	High η
Stationary	8.4	3.5
Time-resolved	7.6	4.6

E. Crossover Point of Rotational Mode of NMC. Since PEO300 consists of about seven –CH_2–CH_2–O– groups, it can be regarded as a polymer made up of twenty on methylene groups. In the low- concentration region, PEO300 molecules are isolated from each other in the solvent. However, PEO300 molecules begin to be packed closely near to the overlap threshold C^*,[13] and PEO300 molecules entangle with each other over C^*. The overlap concentration (C^*) can be evaluated using

$$C^* = \frac{M_w}{N_A\langle s^2\rangle^{3/2}}, \quad (19)$$

where M_w, N_A, and s are the molecular weight, Avogadro's constant, and the end-to-end distance, respectively. The end-to-end distance (s) is roughly estimated by

$$s \simeq N^\nu b, \quad (20)$$

where N, ν, and b are the number of segments (N=21), Flory's exponent[14] (ν=0.588[15]), and the length of one segment (b=1.54 Å), respectively. Thus, one can obtain the overlap concentration of PEO300 (C^*) as 0.64 g ml^{-1}. The crossover point obtained above section, i.e., $\eta^{-1}=1.6\times10^2$ m^2 (Ns)$^{-1}$ for stationary measurement and $\eta^{-1}=2.0\times10^2$ m^2 (Ns)$^{-1}$ for time-resolved measurement, corresponds to the concentration of PEO300 of 0.63 and 0.57 g ml^{-1}, respectively. These crossover points are in good agreement with C^* of PEO300.

Since we selectively excited carbazolyl group by 340 nm, the rotational motion of the NMC molecule, which was detected by a fluorescence depolarization measurement, is not the rotation of the carbazolyl group around the C–N axis (see Fig. 1), because the transition moment of the carbazolyl group is parallel to the C–N axis. We can observe the rotation of the carbazolyl group, for example, around the axis through the carbons of the methylene group and of the 2-position of the naphthyl group. In addition, the rotation of the NMC molecule around an axis vertical to the plane of Fig. 1 can be considered.

In the high-viscosity region of $C > C^*$, the rotation of NMC around the axis vertical to the plane of Fig. 1 would be inhibited because the free volume for the rotation of NMC decreases with increasing concentration of PEO300. Thus, the rotational mode of the carbazolyl or naphthyl group is dominantly detected. In contrast, when the system reaches the low-viscosity region of $C < C^*$, the entire rotation of NMC becomes free. The apparent rate of rotation of NMC becomes fast in the low-viscosity region, as shown Figs. 6

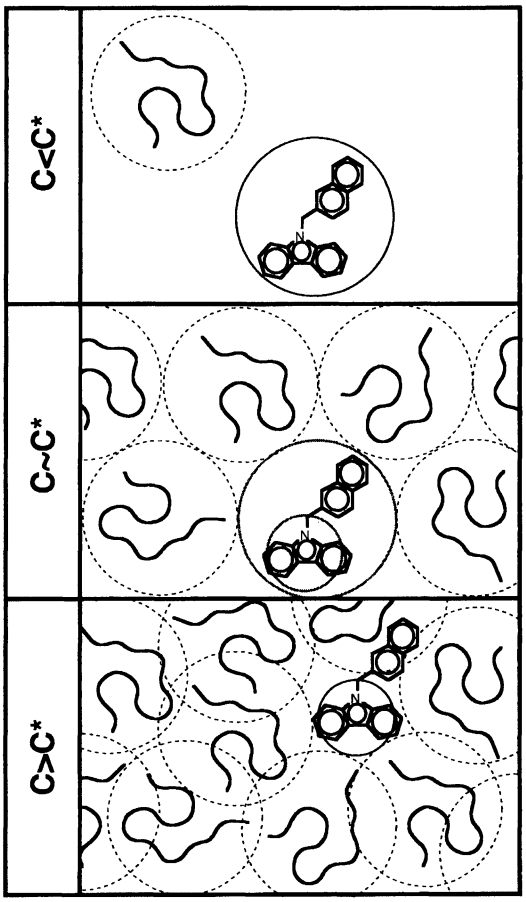

Fig. 9. Schematic representation of rotational behavior of NMC dependent on the concentration of poly(ethylene oxide) in 1,2-dichloroethane/poly(ethylene oxide) mixture.

and 8. We have presumed that the rotational rate of the whole NMC reaches the same order as that of the rotational rate of the carbazolyl group. Namely, the rotational mode of NMC is varied from the whole NMC to the carbazolyl group upon the addition of PEO300 molecules. Figure 9 shows a schematic representation of the rotational behavior of NMC at $C<C^*$, $C\approx C^*$, and $C>C^*$. The effective volume for the rotational motion of NMC changes near $C\approx C^*$. Therefore, the rotational mode detected by the fluorescence depolarization method is associated with the structure of the medium.

Fukumura and Hayashi[16] reported on the rotational behavior of a pyrene sulfonyl group covalently bonded to a protein. When a protein molecule having a pyrene sulfonyl group is in solution, the whole rotational mode is dominantly detected. However, the rotational correlation time becomes small when the protein molecule is adsorbed on a polymer surface. Since a chain of a protein behaves as the medium of a probe molecule, any change in the structure of proteins, which is caused by adsorption on a polymer surface, affects the rotational mode detected dominantly. This result supports our result.

Conclusion

We have shown the rotational behavior of *N*-(2-naphthylmethyl)carbazole molecules in a mixed solvent of 1,2-dichloroethane and poly(ethylene oxide). The rotation of *N*-(2-naphthylmethyl)carbazole is gradually affected by the addition of poly(ethylene oxide). In the low-viscosity region, the radius of gyration of *N*-(2-naphthylmethyl)carbazole was evaluated to be 8.4 Å by a stationary measurement and 7.6 Å by a time-resolved measurement. When the concentration of poly(ethylene oxide) increases to over the overlap concentration, the radius of gyration of *N*-(2-naphthylmethyl)carbazole becomes small: 3.5 and 4.6 Å as estimated by stationary and time-resolved measurements, respectively. Therefore, the rotational mode of NMC is varied from the whole to the carbazolyl group by the addition of PEO300 molecules.

References

1) K. Horie and H. Ushiki, "Hikari Kinou Bunshi No Kagaku," Kodansha, Tokyo (1992).
2) G. Stokes, *Trans. Cambridge Philos. Soc.*, **9**, 5 (1956).
3) A. Einstein, *Am. Phys.*, **19**, 371 (1906).
4) P. Debye, "Polar Molecules," Dover, New York (1929).
5) F. Perrin, *C. R. Acad. Sci. Paris*, **16**, 751 (1924).
6) M. T. Cicerone and M. D. Ediger, *J. Chem. Phys.*, **103**, 5684 (1995).
7) B. Brocklehurst and R. N. Young, *J. Phys. Chem.*, **99**, 40 (1995).
8) A. Srivastava and S. Doraiswamy, *J. Chem. Phys.*, **103**, 6197 (1995).
9) H. Ushiki, K. Horie, and I. Mita, *Chem. Phys. Lett.*, **98**, 285 (1983).
10) P. Wahl, *Biophys. Chem.*, **10**, 91 (1979).
11) T. Nakagawa and Y. Oyanagi, "Saishou Nijyou-hou Niyoru Jikken-Data Kaiseki," Tokyo Daigaku Syuppan-kai, Tokyo (1982).
12) H. Ushiki and I. Mita, *Polym. J.*, **16**, 751 (1984).
13) P. G. de Gennes, "Scaling Concepts in Polymer Physics," Cornell University Press, Ithaca (1979).
14) P. J. Flory, "Principles of Polymer Chemistry," Cornell University Press, Ithaca (1971).
15) M. Doi and A. Onuki, "Koubunshi Butsuri, Souteni Dainamikusu," Iwanami, Tokyo (1992).
16) H. Fukumura and K. Hayashi, *J. Colloid. Interface Sci.*, **135**, 443 (1990).